Channel Estimation for BFDM/OQAM System in Dispersive Time-Varying Channels

Bayarpurev Mongol, Takaya Yamazato, Hiraku Okada, Masaaki Katayama
Graduate School of Engineering, Nagoya University
Furo-cho Chikusa-ku Nagoya-shi, Aichi-ken, 464-8603, JAPAN
Tel/Fax: +81-52-789-2729/ +81-52-789-3173
E-mail: mongol@katayama.nuee.nagoya-u.ac.jp, {yamazato,okada,katayama}@nuee.nagoya-u.ac.jp

***Abstract*— Pulse-shaping OFDM is well-known that it performs well in a mobile environment comparing with conventional OFDM. However, in highly mobile environment intersymbol and intercarrier interferences (ISI/ICIs) increase and can no longer be neglected. These ISI/ICIs deteriorate the performance of the systems. Practically, proper channel equalization and estimation are needed for further improvement of the systems. In this paper, more general case, namely Biorthogonal Frequency Division System based on Offset QAM (BFDM/OQAM) is considered. We first derive analytical equations for the channel statistics. Further, we propose maximum-likelihood channel estimator and its low-complexity versions. The performance analysis shows that the estimators are robust against Doppler spread of the channels.**

I. Introduction

It is well-known that, OFDM signal is robust against time-dispersion, caused by multipath propagation. That is, inter-symbol interfence (ISI) is relatively low in the conventional OFDM signal. However, it is relatively sensitive to frequency dispersion caused by time-variation of the channel. Time-variations corrupt orthogonality of the subcarriers, thus inter-carrier interference (ICI) occurs.

Recently, there has been increased interest in using OFDM systems in a mobile environment. They are considered to be promising candidates for the next generation mobile communications. The mobile environment is characterized by time-frequency dispersion. Signal distortion caused by the time-frequency dispersive channels depends crucially on the time-frequency localization of the pulse-shaping filter[**?**]. For instance, conventional OFDM systems that use rectangular-type pulse with guard interval can prevent ISI, but do not combat ICI. The design of time-frequency well-localized pulse-shaping OFDM filter is, therefore, an active area of research [**?**]-[**?**].

By introducing well-localized transmitter pulse-shapes, it is possible to reduce the ISI/ICIs [**?**]. The performance of such pulse-shaping OFDM systems in dispersive time-varying channels depend critically on the time-frequency localization of the transmitter and receiver filters. Ideally, the system should use time-frequency well-localized transmitter pulse while keeping maximal spectral efficiency. For large number of subcarriers the spectral efficiency ρ of the OFDM system may be approximated by $\rho = 1/(TF)$ symbols per second per Hertz [**?**], here T is a symbol period and F is a subcarrier separation. It is obvious that maximal spectral efficiency is $\rho_{max} = 1$. However, due to Balian-Low theorem [**?**], it is impossible for the OFDM system, based on Quadrature Amplitude Modulation (QAM), to have the well-localized pulses at maximal spectral efficiency [**?**], [**?**].

Numbers of interesting pulse-shaping OFDM systems are proposed recently to deal with the problem. Biorthogonal Frequency Division Multiplexing systems based on Offset QAM (OFDM/OQAM and BFDM/OQAM) allow the construction of well-localized dual pulses at critical sampling (i.e. $TF = 1$), which is desirable in high data-rate applications [**?**], [**?**], [**?**]. The latter relaxes orthogonality condition and uses linearly independent subcarriers. As a result, it allows a broader class of pulse-shapes, particularly the Gaussian transmitter pulse, which has the best time-frequency localization (TFL). Therefore, we can consider BFDM/OQAM as a generalization of pulse-shaping OFDM.

The use of time-frequency well-localized transmitter pulses for BFDM/OQAM systems results in a decrease in ISI/ICI, and the ISI/ICI may be neglected in some practical cases [**?**], [**?**]. However, in highly mobile environments ISI/ICIs increase and can no longer be neglected. A careful investigation of statistical properties of ISI/ICIs and proper equalization and estimation thereof are needed for further improvement of the systems [**?**].

Generally, the channel state information is needed for the construction of robust equalization. Previously proposed robust channel estimators neglect ISI/ICIs [**?**], [**?**]. In this paper, we consider ISI and ICI simultaneously. We first derive optimum maximum-likelihood (ML) estimator for so-called channel parameters, which fully describe the channel state. The ML estimator uses the correlation matrix of the channel parameters. However, calculation of the matrix elements appears to be prohibitively complex. Therefore, we also propose reduced-complexity estimator. Generally, the proposed estimator can be applied to any class of pulse-shaping OFDM systems.

This paper is organized as follows. Section II introduces statistics of the typical mobile wireless channel. Next, Section III briefly reviews the background for BFDM/OQAM system, defines channel parameters, which fully describe the channel state, and discusses their statistics. Then, Section IV presents the proposed ML estimators and analyzes their performance. Finally, Section V discusses numerical study. Here we de-

1-4244-0398-7/06/$20.00 ©2006 IEEE

mostrate that the proposed estimators perform well in the highly mobile environment.

II. MOBILE MULTIPATH CHANNEL

Consider a linear multipath propagation channel characterized by an infinite set of paths with complex amplitudes $\{h_m\}$, delays $\{\tau_m\}$, and incident angles $\{\theta_m\}$ with respect to direction of motion of a mobile station. We make a standard assumption of wide-sense stationary uncorrelated scattering (WSSUS). Further we assume Rayleigh paths with exponentially decaying delay profile with root-mean-square delay spread τ_0:

$$\sum_{m:\tau_m\in(\tau,\tau+d\tau)} \mathbf{E}\{|h_m|^2\} = \frac{1}{\tau_0}e^{-\tau/\tau_0}d\tau \tag{1}$$

where $\mathbf{E}\{\cdot\}$ is the mathematical expectation, τ_0 is root mean square delay spread, τ_m and h_m are the delay and complex amplitude of the m-th path, respectively. In this paper make the following assumption.

Assumption I: For arbitrary interval $[\tau;\tau+d\tau]$ there exist such paths, the delay of which belongs to this interval.

The assumption will approximate a real channel with large number of scatterers, which is typical for practical urban environment. If we denote sum of the complex amplitudes of the paths in *Assumption I* with $h(\tau)$ then WSSUS implies:

$$\mathbf{E}\{h(\tau_1)h^*(\tau_2)\} = \frac{1}{\tau_0}e^{-\tau/\tau_0}\delta(\tau_1-\tau_2) \tag{2}$$

We also assume that the channel has Jakes' Doppler power spectrum. Time variation (i.e. flat fading) of $h(\tau)$ can be expressed as [**?**]:

$$\xi(t) = \xi_c(t) + j\xi_s(t) \tag{3}$$

$$\xi_c(t) = \sqrt{\frac{2}{m_\tau}} \sum_{m:\tau_m\in(\tau,\tau+d\tau)} \cos(2\pi f_d t\cos\alpha_m + \phi_m)$$

$$\xi_s(t) = \sqrt{\frac{2}{m_\tau}} \sum_{m:\tau_m\in(\tau,\tau+d\tau)} \sin(2\pi f_d t\cos\alpha_m + \phi_m)$$

where, α_i and ϕ_i are arrival angle and phase shift of the i-th path, respectively, f_d is the maximum Doppler shift, and m_τ is the number of paths with delay τ_m belong to the interval $[\tau,\tau+d\tau]$. Autocorrelation and crosscorrelation functions of this normalized fading process are given by [**?**]:

$$\begin{aligned} R_{\xi_c\xi_c}(\Delta t) &= \mathbf{E}\{\xi_c(t+\Delta t)\xi_s(t)\} = J_0(2\pi f_d\Delta t) \\ R_{\xi_s\xi_s}(\Delta t) &= \mathbf{E}\{\xi_c(t+\Delta t)\xi_s(t)\} = J_0(2\pi f_d\Delta t) \\ R_{\xi_s\xi_c}(\Delta t) &= R_{\xi_c\xi_s}(\Delta t) = 0 \end{aligned} \tag{4}$$

where, $J_0(\cdot)$ is 0-order Bessel function of the first kind.

III. BFDM/OQAM SYSTEM, ISI/ICI AND CHANNEL PARAMETERS

Here, we review some mathematical background for BFDM/OQAM, analyze the ISI/ICI for the system that occur in the channel described in Section II, and derive second-order statistics for the channel parameters.

A. Biorthogonal Basis and BFDM/OQAM Systems

Let us define a set $\mathbf{G}$ that consists of pairs of the translations and the modulations of a real-valued transmitter pulse $g(t)$:

$$\mathbf{G} = \begin{cases} g^{\mathcal{R}}_{k,l}(t) = g(t-lT)e^{j2\pi Fkt} \\ g^{\mathcal{I}}_{k,l}(t) = g(t-lT+T/2)e^{j2\pi Fkt} \end{cases}$$

where, T is the symbol period, F is subcarrier separation, $N\in\mathbb{N}$ is number of subcarriers and $k,l\in\mathbb{Z}$. From the Gabor theory, $\mathbf{G}$ may form a Riesz basis for a separable Hilbert space only if $TF\geq 1$. For data to be transmitted and received perfectly, in the absence of a channel, elements of $\mathbf{G}$ should be linearly independent (not necessarily be orthogonal). If the elements are orthogonal, the system is called OFDM/OQAM. For any Riesz basis $\mathbf{G}$, there exists unique dual Riesz basis $\mathbf{W}$, such that $\mathbf{G}$ and $\mathbf{W}$ are biorthognal [**?**]. $\mathbf{W}$ also consists of the pairs of translations and modulations of some real-valued pulse $w(t)$:

$$\mathbf{W} = \begin{cases} w^{\mathcal{R}}_{k,l}(t) = w(t-lT)e^{-j2\pi Fkt} \\ w^{\mathcal{I}}_{k,l}(t) = w(t-lT+T/2)e^{-j2\pi Fkt} \end{cases}$$

where $k,l\in\mathbb{Z}$.

$\mathbf{G}$ and $\mathbf{W}$ are dual basis iff the following biorthogonality conditions are satisfied:

$$\Re\{< g^{\mathcal{R}}_{k,l}(t), w^{\mathcal{R}}_{k',l'}(t) >\} = \delta_{k,k'}\delta_{l,l'} \tag{5}$$

$$\Im\{< g^{\mathcal{R}}_{k,l}(t), w^{\mathcal{I}}_{k',l'}(t) >\} = 0 \tag{6}$$

$$\Re\{< g^{\mathcal{I}}_{k,l}(t), w^{\mathcal{R}}_{k',l'}(t) >\} = 0 \tag{7}$$

$$\Im\{< g^{\mathcal{I}}_{k,l}(t), w^{\mathcal{I}}_{k',l'}(t) >\} = \delta_{k,k'}\delta_{l,l'} \tag{8}$$

where, $<\cdot>$ denotes $\mathbf{L}^2$ space inner product,$\Re\{\cdot\}$ and $\Im\{\cdot\}$ denote real and imaginary part, respectively, $\delta_{k,k'}$ denotes the Kronecker delta, and $k,l,k',l'\in\mathbb{Z}$. For more thorough discussion on this topic refer to [3].

The baseband BFDM/OQAM signal can be expressed as:

$$x(t) = \sum_{k=0}^{N-1}\sum_{l=-\infty}^{\infty}\left\{c^{\mathcal{R}}_{k,l}g^{\mathcal{R}}_{k,l}(t) + jc^{\mathcal{I}}_{k,l}g^{\mathcal{I}}_{k,l}(t)\right\} \tag{9}$$

where, T is symbol period, and $c^{\mathcal{R}}_{k,l}$,$c^{\mathcal{I}}_{k,l}$ are real and imaginary parts of the transmitted symbols $c_{k,l}$, respectively. We assume that $c_{k,l}$s are independent and identically distributed (*i.i.d*) random variables. Transmitted signal propagates through mobile multipath channel described in Section 2. Received noisy signal may be written as:

$$s(t) = \sqrt{E_s}\sum_m h_m x(t-\tau_m)\xi_m(t) + n(t) \tag{10}$$

where E_s is signal energy per channel use, $\xi_m(t)$ is flat fading process of the m-th path and $n(t)$ is additive white Gaussian noise (AWGN) within signal bandwidth with the variance $N_0/2$ per complex dimension.

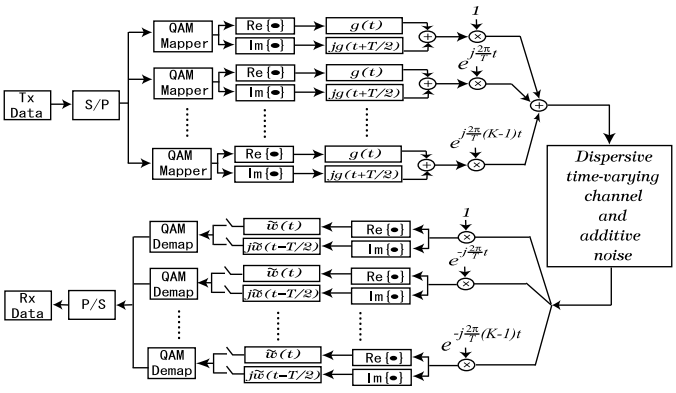

Fig. 1. BFDM/OQAM system, $\tilde{w}(t) = w(-t)$

Demodulation performed at the receiver can be expressed as:

$$d^{\mathcal{R}}_{k',l'} = \Re\{< s(t), w^{\mathcal{R}}_{k',l'}(t) >\} = \quad (11)$$
$$= \int_{-\infty}^{\infty} \Re\left\{s(t)e^{-j2\pi Fk't}\right\} w(t - l'T)dt$$
$$d^{\mathcal{I}}_{k',l'} = \Im\{< s(t), w^{\mathcal{I}}_{k',l'}(t) >\} = \quad (12)$$
$$= \int_{-\infty}^{\infty} \Im\left\{s(t)e^{-j2\pi Fk't}\right\} w(t + \frac{T}{2} - l'T)dt$$

where, $d^{\mathcal{R}}_{k',l'}$,$d^{\mathcal{I}}_{k',l'}$ are the real and imaginary parts of received symbols $d_{k',l'}$, respectively. Block diagram of the BFDM/OQAM system is shown in Fig.1. $\tilde{w}(t) = w(-t)$ can be seen as a matched filter to transmitter pulse $g(t)$.

B. Channel Paramater Statistics

After passing through the time-frequency dispersive channel, the transmitted signal loses its biorthogonality, causing ISI/ICI in the received signal. Therefore, within the *coherence time* of the channel, received symbols in (11) and (12) can be approximated as:

$$d^{\mathcal{R}}_{k,n} = \sum_{i,j}\left\{h^{k,\mathcal{R}}_{i,j,\mathcal{R}}c^{\mathcal{R}}_{k\ominus i,n-j} + h^{k,\mathcal{R}}_{i,j,\mathcal{I}}c^{\mathcal{I}}_{k\ominus i,n-j}\right\} + n^{\mathcal{R}}_{k,n} \quad (13)$$

$$d^{\mathcal{I}}_{k,n} = \sum_{i,j}\left\{h^{k,\mathcal{I}}_{i,j,\mathcal{R}}c^{\mathcal{R}}_{k\ominus i,n-j} + h^{k,\mathcal{I}}_{i,j,\mathcal{I}}c^{\mathcal{I}}_{k\ominus i,n-j}\right\} + n^{\mathcal{I}}_{k,n} \quad (14)$$

where, $\ominus$ is a modulo-N subtraction, $n^{\mathcal{R}}_{k,n}$ and $n^{\mathcal{I}}_{k,n}$ are noise components. $h^{k,\mathcal{R}}_{i,j,\mathcal{R}}$, $h^{k,\mathcal{R}}_{i,j,\mathcal{I}}$, $h^{k,\mathcal{I}}_{i,j,\mathcal{R}}$ and $h^{k,\mathcal{I}}_{i,j,\mathcal{I}}$ are equivalent channel parameters or simply, *channel parameters*. The equivalent channel includes transmitter and receiver filters, as well as the physical medium, i.e. the time-frequency dispersive channel. Except the case $k \neq i$ they present ISI/ICI caused by the channel. Note that even when $k = i$, they show an interference between real and imaginary parts of the same symbol. Channel parameters verify [**?**]:

$$h^{k,\mathcal{R}}_{i,j,\mathcal{R}} = \sqrt{E_s}\int_{-\infty}^{\infty}\Re\left\{\sum_m h_m g(t - jT - \tau_m)\right. \quad (15)$$
$$\left.\cdot\xi_m(t)e^{j2\pi Fi(t-\tau_m)}e^{-j2\pi Fkt}\right\} w(t)dt$$

$h^{k',l',\mathcal{I}}_{k,l,\mathcal{R}}$, $h^{k',l',\mathcal{R}}_{k,l,\mathcal{I}}$ and $h^{k',l',\mathcal{I}}_{k,l,\mathcal{I}}$ can be expressed in the same way.

In Rayleigh fading channels, the channel parameters are zero-mean complex Gaussian random variables. Using Equations (1)-(4), *Assumption I* and noting that $\xi(t)$ and $h(\tau)$ are statistically independent variables, the second order statistics can be derived as [**?**]:

$$\mathbf{E}\{h^{k,\mathcal{R}}_{i,j,\mathcal{R}}h^{k,\mathcal{R}}_{i',j',\mathcal{R}}\} = 2\int_0^{\infty} d\tau\frac{e^{-\tau/\tau_0}}{\tau_0}\iint_{-\infty}^{\infty} dt_1dt_2$$
$$\cdot J_0(2\pi f_d \mid t_1 - t_2 \mid)g(t_1 - lT - \tau)w(t_1)$$
$$\cdot\cos\left[2\pi F\left\{(i-k)t_1 - (i'-k)t_2 - (i-i')\tau\right\}\right]$$
$$g(t_2 - (j'-j)T - \tau)w(t_2) \quad (16)$$

In the same way, the second-order statistics can be derived for all of the other channel parameters.

IV. Maximum-Likelihood Channel Estimator

In this subsection we derive optimum maximum-likelihood (ML) estimator, and its lower complexity versions. We rewrite (13) and (14), approximating summation with its partial sum within a square $-\theta \leq i \leq \theta, -\gamma \leq j \leq \gamma$:

$$d_{k,n} = \sum_{i=-\theta}^{\theta}\sum_{j=-\gamma}^{\gamma}\{a^k_{i,j}c_{k\ominus i,n-j} + b^k_{k',l'}c^*_{k\ominus i,n-j}\} + n_{k,n} \quad (17)$$

where, complex-valued channel parameters $a^k_{i,j} = (h^{k,\mathcal{R}}_{i,j,\mathcal{R}} + h^{k,\mathcal{I}}_{i,j,\mathcal{I}})/2 + j(h^{k,\mathcal{I}}_{i,j,\mathcal{R}} - h^{k,\mathcal{R}}_{i,j,\mathcal{I}})/2$ and $b^k_{k',l'} = (h^{k,\mathcal{R}}_{i,j,\mathcal{R}} - h^{k,\mathcal{I}}_{i,j,\mathcal{I}})/2 + j(h^{k,\mathcal{I}}_{i,j,\mathcal{R}} + h^{k,\mathcal{R}}_{i,j,\mathcal{I}})/2$.

Equation (17) has $2(2\theta + 1)(2\gamma + 1)$ unknown complex-valued channel parameters per subcarrier. We define a channel state vector $\mathbf{h}$ that consists of the complex-valued channel parameters. Then, log-likelihood function for the channel state vector $\mathbf{h}$ can be expressed as:

$$\Psi(\mathbf{h}) = \frac{1}{2}\mathbf{h}^*\bar{\mathbf{R}}\mathbf{h} +$$
$$\sum_{k'=0}^{N-1}\frac{1}{N_0}|d_{k',n} - \sum_{i,j}(a^{k'}_{i,j}c_{k'\ominus i,n-j} + b^{k'}_{i,j}c^*_{k'\ominus i,n-j})|^2 \quad (18)$$

where $\bar{\mathbf{R}} = \mathbf{R}^{-1}$ is the inverse of the channel parameter crosscorrelation matrix.

The solution for (20) is ommitted in this paper. It uses inversion of the matrix $\mathbf{R}$. However, calculation of elements of $\mathbf{R}$ is numerically complex. Thus, we propose low-complexity versions that requires calculation of near-the-diagonal elements.

A. Low-complexity Estimator

In this subsection derive suboptimal low complexity estimators for the channel state vector. In the above discussed optimal (assuming the noise is white) ML estimator, the calculation of elements of the channel parameter correlation matrix $\mathbf{R}$ is prohibitively complex. Therefore, in the training sequence impulses are used. We choose separations of the training impulses in the time-frequency lattice, so that every single received symbol during training period will be interfered by

only one impulse. For convenience, we derive ML estimates for real-valued channel parameters.

First we derive so-called single-term estimator. We assume that a pulse with amplitude 1 (or j) is transmitted at node (α, β) on the time-frequency lattice, i.e. $c_{\alpha,\beta} = 1$ and that any received symbol is interfered by only one transmitted symbol. That is, all of the adjacent symbols $c_{\alpha+k,\beta+l}$ are equal to zero, at least within the square $-2\psi \le k \le 2\psi$ and $-2\phi \le l \le 2\phi$. Then, from (13) and (14), it is obvious that:

$$d^{\mathcal{R}}_{\alpha+k,\beta+l} = h^{\alpha-k,\mathcal{R}}_{k,l,\mathcal{R}} + n^{\mathcal{R}}_{\alpha+k,\beta+l} \tag{19}$$

$$d^{\mathcal{I}}_{\alpha+k,\beta+l} = h^{\alpha-k,\mathcal{I}}_{k,l,\mathcal{R}} + n^{\mathcal{I}}_{\alpha+k,\beta+l} \tag{20}$$

ML estimates of the channel parameters in (22) and (23) can be checked:

$$\begin{aligned}\hat{h}^{\alpha-k,\mathcal{R}}_{k,l,\mathcal{R}} &= \frac{d^{\mathcal{R}}_{\alpha+k,\beta+l}\sigma_{h^{\alpha-k,\mathcal{R}}_{k,l,\mathcal{R}}}}{N_0 + \sigma_{h^{\alpha-k,\mathcal{R}}_{k,l,\mathcal{R}}}},\ \sigma_{h^{\alpha-k,\mathcal{R}}_{k,l,\mathcal{R}}} = \mathbf{E}\{{h^{\alpha-k,\mathcal{R}}_{k,l,\mathcal{R}}}^2\} \\ \hat{h}^{\alpha-k,\mathcal{I}}_{k,l,\mathcal{R}} &= \frac{d^{\mathcal{I}}_{\alpha+k,\beta+l}\sigma_{h^{\alpha-k,\mathcal{I}}_{k,l,\mathcal{R}}}}{N_0 + \sigma_{h^{\alpha-k,\mathcal{I}}_{k,l,\mathcal{R}}}},\ \sigma_{h^{\alpha-k,\mathcal{I}}_{k,l,\mathcal{R}}} = \mathbf{E}\{{h^{\alpha-k,\mathcal{I}}_{k,l,\mathcal{R}}}^2\}\end{aligned} \tag{21}$$

In the same manner, ML estimates for $h^{\alpha-k,\mathcal{R}}_{k,l,\mathcal{I}}$ and $h^{\alpha-k,\mathcal{I}}_{k,l,\mathcal{I}}$ can be derived.

We may also derive double-term estimator. Let us assume that a pulse with amplitude $1 + j$ is trasmitted at node α, β on the time-frequency lattice, and the other conditions are the same as previous. Then, received symbol is expressed as:

$$d^{\mathcal{R}}_{\alpha+k,\beta+l} = h^{\alpha-k,\mathcal{R}}_{k,l,\mathcal{R}} + h^{\alpha-k,\mathcal{R}}_{k,l,\mathcal{I}} + n^{\mathcal{R}}_{\alpha+k,\beta+l} \tag{22}$$

$$d^{\mathcal{I}}_{\alpha+k,\beta+l} = h^{\alpha-k,\mathcal{I}}_{k,l,\mathcal{R}} + h^{\alpha-k,\mathcal{I}}_{k,l,\mathcal{I}} + n^{\mathcal{I}}_{\alpha+k,\beta+l} \tag{23}$$

and, ML estimates can be checked:

$$\begin{aligned}\hat{h}^{\alpha-k,\mathcal{R}}_{k,l,\mathcal{R}} &= \frac{2d^{\mathcal{R}}_{\alpha+k,\beta+l}(\sigma_1 + \rho\sqrt{\sigma_1\sigma_2})}{N_0 + 2(\sigma_1 + \sigma_2 + \rho\sqrt{\sigma_1\sigma_2})} \\ \hat{h}^{\alpha-k,\mathcal{R}}_{k,l,\mathcal{I}} &= \frac{2d^{\mathcal{R}}_{\alpha+k,\beta+l}(\sigma_2 + \rho\sqrt{\sigma_1\sigma_2})}{N_0 + 2(\sigma_1 + \sigma_2 + \rho\sqrt{\sigma_1\sigma_2})}\end{aligned} \tag{24}$$

where, $\sigma_1 = \mathbf{E}\{{h^{\alpha-k,\mathcal{R}}_{k,l,\mathcal{R}}}^2\}$, $\sigma_2 = \mathbf{E}\{{h^{\alpha-k,\mathcal{R}}_{k,l,\mathcal{I}}}^2\}$,and $\rho = \mathbf{E}\{h^{\alpha-k,\mathcal{R}}_{k,l,\mathcal{R}} h^{\alpha-k,\mathcal{R}}_{k,l,\mathcal{I}}\}/\sqrt{\sigma_1\sigma_2}$. Other channel parameter estimates can be derived in the same way.

Operational complexity of ML estimator in (21) and (24) are considerably low compared with the optimum estimator. However, the training sequence uses pulses that separated in the time-frequency lattice. This degrades the efficiency of the estimation. To increase the efficiency, we reduce the separations between impulses. In that case, received symbols would be interfered from other impulses, which will result in an estimation error. The optimal point should be carefully investigated. We can see that the single-term estimator in (21) uses twice longer training sequence than the double-term estimator in (24).

B. Mismatch Analysis for the Low-complexity Estimators

We derive lower bound on the total mean-square error(MSE) for the channel estimates. The total MSE is defined as:

$$\begin{aligned}MSE(\psi,\phi) = \sum_{i,j} \mathbf{E}\{&(h^{k,\mathcal{R}}_{i,j,\mathcal{R}} - \hat{h}^{k,\mathcal{R}}_{i,j,\mathcal{R}})^2 + (h^{k,\mathcal{I}}_{i,j,\mathcal{R}} - \hat{h}^{k,\mathcal{I}}_{i,j,\mathcal{R}})^2 \\ &+ (h^{k,\mathcal{R}}_{i,j,\mathcal{I}} - \hat{h}^{k,\mathcal{R}}_{i,j,\mathcal{I}})^2 + (h^{k,\mathcal{I}}_{i,j,\mathcal{I}} - \hat{h}^{k,\mathcal{I}}_{i,j,\mathcal{I}})^2\}\end{aligned}$$

The total MSE is lower bounded with $MSE(N/2,\infty)$, that is, no other impulse is interfered into the received symbol. For the single-term case, it is straightforward to see that:

$$\begin{aligned}MSE(N/2,\infty) = N_0 \sum_{i,j} \Bigg(&\frac{\sigma^1_{i,j}}{N_0 + \sigma^1_{i,j}} + \\ &+ \frac{\sigma^2_{i,j}}{N_0 + \sigma^2_{i,j}} + \frac{\sigma^3_{i,j}}{N_0 + \sigma^3_{i,j}} + \frac{\sigma^4_{i,j}}{N_0 + \sigma^4_{i,j}} \Bigg)\end{aligned} \tag{25}$$

where, $\sigma^1_{i,j} = \mathbf{E}\{{h^{k,\mathcal{R}}_{i,j,\mathcal{R}}}^2\}$, $\sigma^2_{i,j} = \mathbf{E}\{{h^{k,\mathcal{R}}_{i,j,\mathcal{I}}}^2\}$, $\sigma^3_{i,j} = \mathbf{E}\{{h^{k,\mathcal{I}}_{i,j,\mathcal{R}}}^2\}$, and $\sigma^4_{i,j} = \mathbf{E}\{{h^{k,\mathcal{I}}_{i,j,\mathcal{I}}}^2\}$.

For the double-term case, $MSE(N/2,\infty)$ verifies:

$$\begin{aligned}MSE(N/2,\infty) = &\frac{\sigma^1_{i,j}\sigma^2_{i,j}(16\sqrt{\sigma^1_{i,j}\sigma^2_{i,j}}(1-{\rho^{12}_{i,j}}^2) + 8N_0)}{(N_0 + 2(\sigma^1_{i,j} + \sigma^2_{i,j}))^2} \\ &\frac{(\sigma^1_{i,j} + \sigma^2_{i,j})(8N_0\sqrt{\sigma^1_{i,j}\sigma^2_{i,j}} + N_0^2) + N_0({\sigma^1_{i,j}}^2 + {\sigma^2_{i,j}}^2)}{(N_0 + 2(\sigma^1_{i,j} + \sigma^2_{i,j}))^2} \\ &\frac{\sigma^3_{i,j}\sigma^4_{i,j}(16\sqrt{\sigma^3_{i,j}\sigma^4_{i,j}}(1-{\rho^{34}_{i,j}}^2) + 8N_0)}{(N_0 + 2(\sigma^3_{i,j} + \sigma^4_{i,j}))^2} \\ &\frac{(\sigma^3_{i,j} + \sigma^4_{i,j})(8N_0\sqrt{\sigma^3_{i,j}\sigma^4_{i,j}} + N_0^2) + N_0({\sigma^3_{i,j}}^2 + {\sigma^4_{i,j}}^2)}{(N_0 + 2(\sigma^3_{i,j} + \sigma^4_{i,j}))^2}\end{aligned} \tag{26}$$

where, $\rho^{12}_{i,j} = \mathbf{E}\{h^{k,\mathcal{R}}_{i,j,\mathcal{R}} h^{k,\mathcal{R}}_{i,j,\mathcal{I}}\}/\sqrt{\sigma_1\sigma_2}$ and $\rho^{34}_{i,j} = \mathbf{E}\{h^{k,\mathcal{I}}_{i,j,\mathcal{R}} h^{k,\mathcal{I}}_{i,j,\mathcal{I}}\}/\sqrt{\sigma_3\sigma_4}$.

V. Numerical Simulation

The total MSE performance of the proposed estimators is evaluated by computer simulation. The simulation BFDM/OQAM system is constructed at maximal spectral efficiency, i.e. $TF = 1$. Transmitter filter uses Gaussian pulse and receiver matched filter uses corresponding dual pulse discussed in Section III. Digital mapping is 16QAM. No guard interval is used and symbol period is $T = 3.2\mu s$. The dispersive time-varying channel is the Rayleigh fading channel with Jakes Doppler Spectrum as described in Section II. Maximum Doppler shift of the channel is $f_d \in [0Hz, 700Hz]$, which corresponds to vehicle speed of $v \in [0km/h, 300km/h]$, at carrier frequency $f_c = 2.5GHz$. The channel has 200 paths and exponentially decaying multipath intensity profile. Root-mean-square delay is $\tau_0 = 0.5\mu s$. 500 simulation runs are averaged to plot the total MSE.

Fig.2 shows the total MSE of the channel estimators versus the speed of the vehicle, when SNR=30dB, the rms delay spread is $\tau_0 = 0.5\mu s$. Dotted curves show the performance

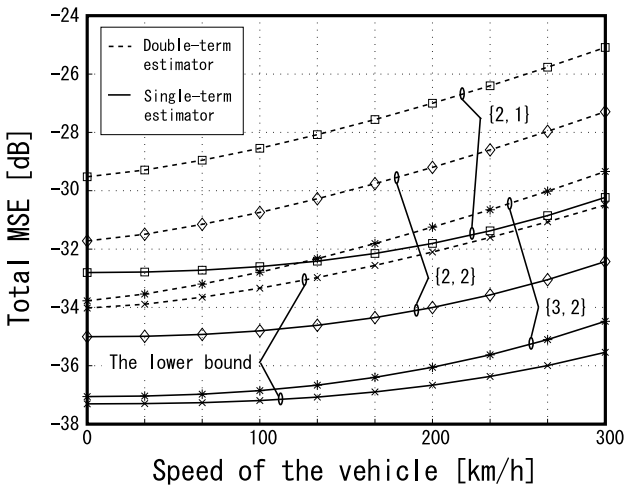

Fig. 2. The total MSE of channel estimators versus the speed of the vehicle, when SNR=30dB, the rms delay $\tau_0 = 0.5\mu s$, time-frequency separation between impulses $[\psi, \phi] = [3, 2]$, $[2, 2]$, and $[2, 1]$

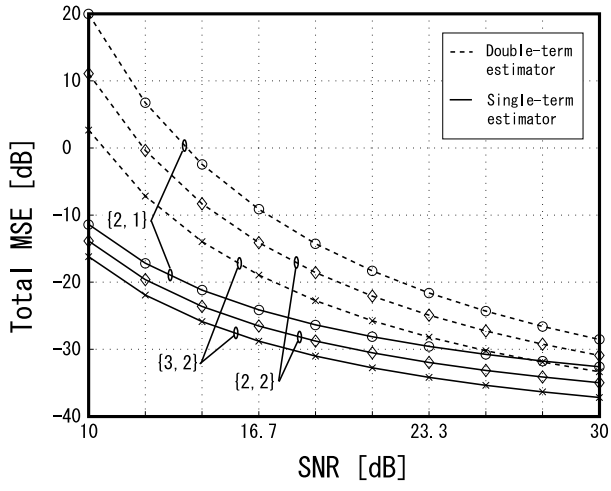

Fig. 3. The total MSE of channel estimators versus SNR, when the speed of the vehicle is $100km/h$, the rms delay is $\tau_0 = 0.5\mu s$, time-frequency separations between impulses are $[\psi, \phi] = [3, 2]$, $[2, 2]$, and $[2, 1]$

of the double-term estimator and solid curves the single-term estimator. The lower bound curves $- \times -$ is achieved by evaluating $MSE(N/2, \infty)$ in Subsection IV. B. The time-frequency separations $[\psi, \phi]$ between impulses in the training sequence are $[3, 3]$ (curves $- * -$), $[2, 2]$ (curves $- \diamond -$), and $[2, 1]$ (curves $-\Box-$). It can be observed that for the single-term estimator, the total MSE at speed $300km/h$ is $2.2dB$ higher than the one achieved at the stationary channel. For the double-term estimator the difference is $4.2dB$.

Fig. 3. shows the total MSE versus SNR, when speed of vehicle is $100km/h$, the rms delay spread is $\tau_0 = 0.5\mu s$. We can observe that the performance of the double-term estimator deteriorates faster, when noise increases. Indeed, at $SNR = 10dB$ the total MSE difference between the estimators is $20dB$ when $[\psi, \phi] = [3, 2]$.

VI. Conclusion

In this paper we have proposed low-complexity estimators for BFDM/OQAM systems in the dispersive time-varying channels. The estimators employ impulses as the training sequence. The impulses are 1 or j for single-term estimator and $1+j$ for double-term estimator. The single-term estimator, thus, uses twice longer training sequence.

We have numerically analyzed the total MSE performance of the estimators. The results show that at time-frequency separation between impulses $[\psi, \phi] = [3, 2]$, the performance approaches theoretical lower bound. In a low-noise environment with $SNR = 30dB$, the total MSE of single-term estimator is $2\ 4dB$ lower than that of double-term estimator. When noise increases, the performance of the double-term estimator deteorates faster.

References

[1] T.Strohmer, and S.Beaver, "Optimal OFDM design for time-frequency dispersive channels," IEEE Trans. Commun., vol. 51, no. 7, pp. 1111–1122, Jul. 2003.

[2] A.Vahlin, and N.Holte, "Optimal finite duration pulses for OFDM," IEEE Trans. Commun., vol. 44, no. 5, pp. 10–14, Jan. 1996.

[3] H. Bölcskei, "Orthogonal frequency division multiplexing based on offset qam," in *Advances in Gabor Analysis*, H. G. Feichtinger and T. Strohmer, Birkhäuser, 2002.

[4] G.D.Schafhuber, and F.Hlawatsch, "Pulse-shaping OFDM/BFDM systems for time-varying channels: ISI/ICI analysis, optimal pulse design, and efficient implementation," Proc. PIMRC, vol. 3, pp. 1012–1016, Sept. 2002.

[5] H.G.Feichtinger, and T.Strohmer, *Gabor Analysis and Algorithms, Theory and Applications*, Birkhaüser, 1998.

[6] G.Kunyniok, and T.Strohmer, "Wilson bases for general time-frequency lattices," SIAM J. Math. Anal., vol. 37, no. 3, pp. 685-711, Nov. 2005.

[7] W.Kozek, and A.Molisch, "Nonorthogonal pulseshapes for multicarrier communications in doubly dispersive channels," IEEE J. Select. Areas Comm., vol.16, pp.1579–1589, Aug. 1998.

[8] Y. Li, L.J.Cimini, and N.R.Sollenberger, "Robust Channel Estimation for OFDM Systems with Rapid Dispersive Fading Channels, " IEEE Trans. Commun., vol. 46, no.7, pp. 902-915, Jul. 1998.

[9] D. Schafhuber, and G. Matz "MMSE and Adaptive Prediction of Time-Varying Channels for OFDM Systems," IEEE Trans. Commun., vol. 4, no. 2, pp. 593–602, Mar. 2005.

[10] B.Mongol, T.Yamazato, H. Okada, and M.Katayama, "On the second-order statistics of the channel parameters for BFDM/OQAM systems," ISWCS2005 Proc., Sep. 2005.

[11] W.C.Jakes, *Microwave Mobile Communications*, IEEE Press, 1994.

[12] R.Haas, and J.Belfiore, "A time-frequency wel-localized pulse for multiple carrier transmission," Wireless Pers. Comm., vol. 5, pp. 1–18, Jul. 1997.

[13] M.J.Bastiaan, "Gabor's espansion and the zak transform for continuous-time and discrete-time signals: Critical sampling and rational oversampling," Eindhoven University of Technolody Research Reports, Dec. 1995.

[14] H.G.Feichtinger, and T.Strohmer, *Advances in Gabor Analysis*, Birkhäuser, 2002.

[15] H.Bölcskei, "Discrete zak transform, polyphase transforms, and applications," IEEE Trans. Sig. Proc.,vol. 45, no. 4, pp. 851-866, Aprl. 1997.

Acknowledgement

This work was supported in part by the The 21st Century COE Program by the Ministry of Education, Culture, Sports, Science and Technology in Japan, and Fujitsu Laboratory.